

Modulation of flat-band voltage on H-terminated silicon-on-insulator pseudo-metal-oxide-semiconductor field effect transistors by adsorption and reaction events

Girjesh Dubey,^{1,2} Federico Rosei,^{2,3} Gregory P. Lopinski^{1,a)}

¹Steacie Institute for Molecular Sciences, National Research Council, 100 Sussex Drive, Ottawa, Ontario K1A 0R6, Canada

²INRS-EMT, Université du Québec, 1650 Boul. Lionel-Boulet, Varennes, Québec J3X 1S2, Canada

³Center for Self-Assembled Chemical Structures, McGill University, 801 Sherbrooke Street West, Montréal, Québec H3A 2K6, Canada

(Received 2 December 2010; accepted 21 March 2011; published online 18 May 2011)

Accumulation mode pseudo-MOSFETs formed on hydrogen terminated silicon-on-insulator (SOI-H) were used to probe molecular adsorption and reaction events. Current-voltage characteristics of such *n*-channel devices are found to be sensitive to the environment, with the accumulation threshold voltage, or flat-band voltage, exhibiting large reversible changes upon cycling between ambient atmosphere, high vacuum ($<10^{-5}$ Torr), and exposure to water and pyridine vapor at pressures in the Torr range. The field-effect mobility is found to be comparatively less affected through these transitions. Oxidation of the H-terminated surface in ambient conditions leads to irreversible shifts in both the flat-band voltage and the field-effect mobility. A photochemical gas phase reaction with decene is used to form a decyl monolayer on the SOI(100)-H surface. Formation of this monolayer is found to result in a relatively small shift of the threshold voltage and only a slight degradation of the field effect mobility, suggesting that alkyl monolayer dielectrics formed in this way could function as good passivating dielectrics in field effect sensing applications. © 2011 American Institute of Physics. [doi:10.1063/1.3583559]

I. INTRODUCTION

Transport properties at semiconductor surfaces are dramatically altered by adsorption and reaction events, which result in charge redistribution at the interface.^{1–6} Hydrogen-terminated silicon-on-insulator (SOI-H) has been shown to be an interesting model system for investigating this sensitivity to surface processes.^{7–9} The architecture of SOI substrates facilitates the formation of a pseudo-MOS transistor (Ψ -MOSFET) simply by making point contacts to the top silicon layer and using the silicon substrate as a gate.¹⁰ As this allows the recording of FET-like characteristics without the need for device fabrication, the Ψ -MOSFET has become a mainstream tool for rapid and nondestructive characterization of SOI wafers.^{11–14} The application of this approach to the monitoring of surface processes is still in its infancy. Control over the inversion threshold voltage ($V_{TH,inv}$) of FETs formed on SOI substrates was demonstrated initially for molecular monolayers formed on oxidized silicon.¹⁵ More recently, the grafting of layers of aromatic molecules with a range of substituents to SOI(111)-H via the reduction of diazonium salts has been used to demonstrate shifts in $V_{TH,inv}$ in accordance with the electron donor/acceptor character of the ligand.^{7,16} The use of photoactive molecules to modulate device properties has also been investigated.¹⁷ Although these later studies used H-terminated silicon as the starting point for forming molecular layers, the device

properties of this surface and its sensitivity to adsorption events were not investigated.

Here we employ the point contact Ψ -MOSFET technique to SOI(100)-H substrates and report significant modulation of the electrical properties caused by simply changing the gaseous environment. Moderately doped ($\sim 10^{15}$ cm⁻³) *n*-type samples with film thickness $d = 150$ to 200 nm are used. The current-voltage characteristics of the Ψ -MOSFETs are used to extract the “threshold voltage” to activate an accumulation *n*-channel ($V_{TH,acc}$) at the device layer/buried oxide interface, which we designate interchangeably as the “flat-band voltage” (V_{FB}). An important parameter in the characterization of FETs, this is the gate voltage required to flatten the bands in the device layer and the threshold point at which a large onset in current is measured as the bands are driven further into accumulation. Changes in V_{FB} are observed upon operation in ambient conditions, in high vacuum, and under controlled exposure to pure H₂O. Adsorption of water is found to shift V_{FB} to more negative values, corresponding to an increase in current at a fixed gate voltage and suggesting that the water induces a positive surface charge. Even larger effects are induced by exposure to pyridine (C₅H₅N). The Ψ -MOSFET was also used to observe irreversible changes associated with the ambient oxidation of the H-terminated surface. Passivation of the H-terminated surface via molecular monolayer formation has also been investigated. A recently developed gas phase photochemical method is found to be a simple and compatible means for the covalent attachment of alkyl chains to the Si(100)-H surface. This process is found to maintain the low density of

^{a)}Author to whom correspondence should be addressed. Electronic mail: Gregory.Lopinski@nrc-cnrc.gc.ca.

electrically active defects typical of the H-terminated surface, suggesting that alkyl monolayers formed in this way could be useful as ultrathin dielectrics for sensing applications.

II. EXPERIMENTAL DETAILS

Separation by implantation of oxygen (SIMOX) substrates from IBIS with buried oxide (BOX) thickness $d_{\text{box}} = 377$ nm and active Si(100) layer thicknesses $d = 150$ nm (*n*-type film/*p*-type substrate) and $d = 200$ nm (*n*-type film/*n*-type substrate) cut to $\sim 20 \times 10$ mm were used.¹⁸ The average carrier density in the top Si film was on the order of $n_b = 1 \times 10^{15} \text{ cm}^{-3}$, determined from Hall effect and sheet resistance measurements. The native oxide was cleaned in piranha solution (3:1 $\text{H}_2\text{SO}_4:\text{H}_2\text{O}_2$) at 120°C for 20 min, rinsed in Milli-Q water ($18 \text{ M}\Omega \cdot \text{cm}$), and then etched in dilute HF (2%) for 2 min. *Hazards:* Piranha solution should be handled with caution, using the appropriate protective measures, and kept isolated from other organic substances. Protective measures and caution should be exercised when handling HF solutions. Tungsten probes were used to make electrical contact with ~ 1 mm sized eutectic gallium indium (EGaIn) drops, which were used to form the source and drain contacts to the H-terminated surface. Contacts were separated by < 5 mm. The substrate back-contact was formed by applying EGaIn to the HF etched surface. The source was the signal ground. A drain-to-source voltage (V_D) and gate-to-source voltage (V_G) were applied, and the drain current (I_D) and leakage¹⁹ from gate to source (I_{GS}) were monitored as a function of time and gate bias using two Keithley 2400 source-measure units. The sample was mounted in a small turbo pumped high vacuum system (base pressure up to 10^{-7} Torr) designed for carrying out electrical measurements during controlled exposure to various gases, as described elsewhere.^{8,20}

Decyl monolayers were formed via a recently reported gas phase photochemical route.²¹ H-terminated samples were quickly transferred to a small vacuum chamber with a sorption pump (base pressure $< 10^{-4}$ Torr). The chamber was equipped with a UV transparent sapphire port allowing 60% transmission at 190 nm as measured by a spectrophotometer. Freeze-pump thawed 1-decene vapor (~ 1 Torr) was leaked into the chamber and irradiated with a Hg-Ne spectral calibration lamp (Oriel 6035) for 10 min. Attenuated total reflection Fourier transform infrared spectroscopy (ATR-FTIR) was used to confirm monolayer formation. FTIR spectra were obtained on Si(100) ATR elements (25 mm long and 1 mm thick, with 45° bevels, obtained from Harrick Scientific). Spectra were acquired using a N_2 -purged Nicolet MAGNA-IR spectrometer equipped with a HgCdTe detector. The resolution was set to 4 cm^{-1} . Piranha cleaned chemical oxide (SiO_2) was used to obtain the background spectrum for the Si(100)-H surface, whereas the Si(100)-H spectrum was used as the background to obtain the spectrum of the decyl modified Si(100)-C10 surface.

III. RESULTS AND DISCUSSION

A. Physisorption modulates V_{FB} reversibly

The output characteristics $I_D(V_D, V_G)$ of a SOI-H *n*-channel Ψ -MOSFET operating in accumulation mode,

measured under vacuum and during exposure to water vapor, are shown in Fig. 1(a). Exposure to water vapor is seen to have a significant effect on the FET characteristics, increasing the current at a given gate voltage. This can be seen clearly by comparing the characteristics at $V_G = 0$ V, as the device is “off” under vacuum whereas significant current is seen when the device is exposed to water vapor. This is further apparent from Fig. 1(b), in which the drain current in saturation ($I_{D,\text{sat}}$) is plotted versus the gate voltage for the SOI-H Ψ -MOSFET in three different environments: (1) ambient, (2) vacuum, and (3) under 7 Torr of water vapor.

Before a formal analysis, it is already evident that the flat-band shifts are large enough to be estimated by visual inspection of the data in Fig. 1. For instance, a ~ 2 V difference between vacuum and water exposure is clearly observable by comparing adjacent sets of I - V traces in Fig. 1(a), and it is also apparent from the separation of saturation curves along the V_G -axis shown in Fig. 1(b). Analytically, the Ψ -MOSFET characteristics in saturation and linear (triode) modes of operations are analogous to the standard MOS transistor.¹¹ In the saturation regime $V_D > V_G - V_{\text{FB}}$, the drain current is properly described by $I_{D,\text{sat}} = 1/2 \beta_{\text{sat}} \cdot (V_G - V_{\text{FB}})^2$ as plotted in Fig. 1(b). Plots of this type can be fitted with a two-parameter parabolic equation to determine V_{FB} and the gain factor $\beta_{\text{sat}} = f_g \mu_{\text{sat}} C_{\text{box}}$. This stretch factor incorporates a geometric coefficient f_g ,

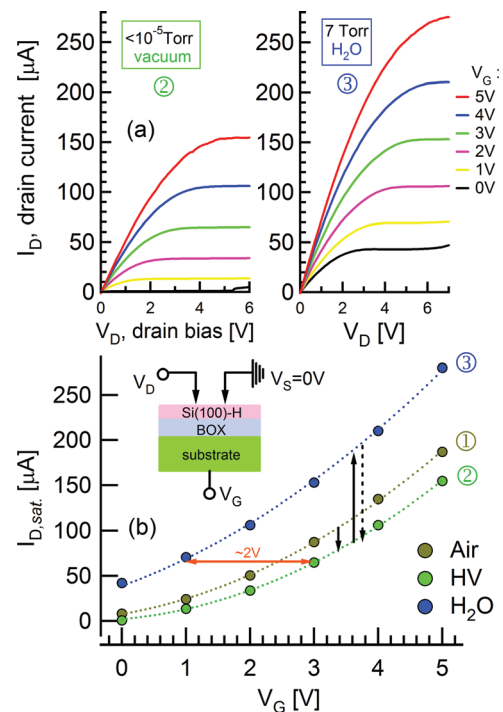


FIG. 1. (Color online) (a) Comparison of drain current (I_D) vs drain voltage (V_D) of *n*-type (100) H-Terminated SIMOX 150 nm in thickness operating in accumulation mode, under high vacuum ($< 10^{-5}$ Torr) and 7 Torr H_2O (g) environments. (b) I_D in saturation vs V_G from (1) initially ambient to (2) $< 10^{-5}$ Torr high-vacuum to (3) 7 Torr water exposure, showing that the stretch factor β_{sat} , which is proportional to a mobility-capacitance product $\mu_{\text{sat}} C_{\text{box}}$, is practically unchanged between transitions. However, the relative change in V_{FB} is extremely sensitive to H_2O coverage, spanning ~ 2 V. The dotted lines are parabolic fits used for parameter extraction. A schematic of the pseudo-MOSFET is shown in the inset.

representing the actual aspect ratio of the channel formed, which was not measured in this study. Importantly, β_{sat} directly relates to a mobility-capacitance product $\mu_{\text{sat}}C_{\text{box}}$. The buried oxide capacitance per unit area is $C_{\text{box}} = \epsilon_0\epsilon_{\text{box}}/d_{\text{box}} = 9.2 \text{ nF/cm}^2$ using the relative permittivity $\epsilon_{\text{box}} = 3.9$ and thickness $d_{\text{box}} = 377 \text{ nm}$. It should be noted that in this model the high-field effective electron mobility μ_{sat} is in general influenced by many factors, including the series resistance of the contacts, as well as the lateral and vertical fields applied by the drain and gate biases, which cause mobility-attenuation.¹¹

The set of parabolas in Fig. 1(b) are observed to have similar shapes; they can be practically superimposed onto one another via simple horizontal translations (corresponding to flat-band shifts) parallel to the V_G -axis. This is quantified by extracting similar stretch factors in the three environments $\beta_{\text{sat}}^{(1)} = 9.6 \pm 0.2 \text{ } \mu\text{A/V}^2$, $\beta_{\text{sat}}^{(2)} = 9.7 \pm 0.2 \text{ } \mu\text{A/V}^2$, and $\beta_{\text{sat}}^{(3)} = 8.7 \pm 0.3 \text{ } \mu\text{A/V}^2$, corresponding to an average $\langle\beta_{\text{sat}}\rangle = 9.3 \pm 0.6 \text{ } \mu\text{A/V}^2$. This indicates that the product $\mu_{\text{sat}}C_{\text{box}}$ remains essentially constant in the three environments, and hence μ_{sat} itself is largely unaffected between transitions, as C_{box} is not expected to change. Based on comparing their I - V characteristics with four-probe measurements, the geometric coefficient has been reported to be $f_g = 0.75$ for a range of probe separations $< 5 \text{ mm}$,¹¹ similar to that used here. Using this value of f_g yields an estimated apparent mobility of $\langle\mu_{\text{sat}}\rangle \approx 1360 \pm 80 \text{ cm}^2/\text{V} \cdot \text{s}$.

In contrast to the stretching factor, the flat-band voltage is highly sensitive to the chemical environment: $V_{\text{FB}}^{(1)} = -1.3 \pm 0.05 \text{ V}$, $V_{\text{FB}}^{(2)} = -0.7 \pm 0.04 \text{ V}$, and $V_{\text{FB}}^{(3)} = -3.0 \pm 0.1 \text{ V}$. Furthermore, the sample can be cycled between vacuum and water-exposed states reversibly—(2) \leftrightarrow (3)—reproducing the same values for V_{FB} and β_{sat} in each cycle. This indicates that water adsorption on the H-terminated surface is a reversible process that does not degrade the electronic properties.^{22,23}

The surprisingly large effects induced by water are exceeded by those seen with other donor-type gases. Pyridine exposure at similar pressures to water (7 Torr) increased the channel conductivity significantly enough to suppress saturation at the same bias conditions used for water as in Fig. 1(a). However, the relative gating strength could still be compared in the linear mode of operation, as shown in Figs. 2(a) and 2(b), and resulted in similar parameter extraction and the same trends found for the quadratic regime in Fig. 1(b). Comparison of the flat-band voltages extracted in the linear region is illustrated in Fig. 2(a) at each of the stages—(1) ambient, (2) vacuum, (3) water, and (4) pyridine—and the corresponding I_D - V_G relationships are provided in Fig. 2(b).

In the triode regime, the dependence of the drain current ($I_{D,\text{lin}}$) is linear in gate voltage, described by $I_{D,\text{lin}} = a \cdot V_G + b$, with slope $a = \beta_{\text{lin}}V_D$ and intercept $b = \beta_{\text{lin}}V_D(V_{\text{FB}} + 1/2 V_D)$. Analogous to the case for saturation, $\beta_{\text{lin}} = f_g\mu_{\text{lin}}C_{\text{box}}$ is proportional to a mobility-capacitance product, where μ_{lin} is the low-field effective electron mobility, also dependent on gate bias and contact resistance.¹¹ The slopes and intercepts from Fig. 2(b) are used to determine $\beta_{\text{lin}} = a/V_D$ and $V_{\text{FB}} = -1/2 V_D - b/a$. Immediately observable in Fig. 2(b), all four lines are parallel but vary significantly in intercept, which results

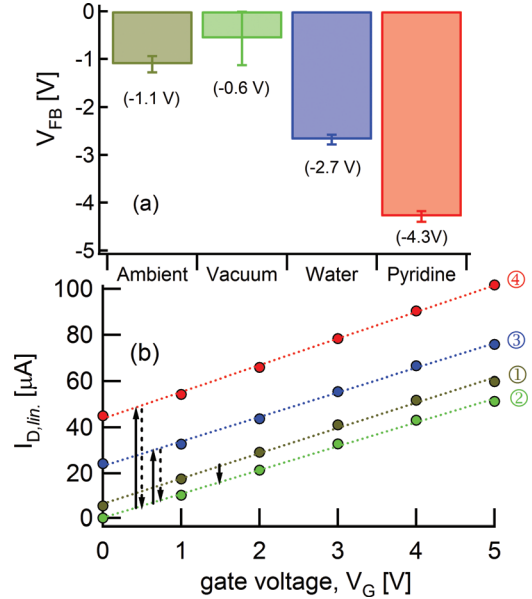


FIG. 2. (Color online) SOI(100)-H (a) flat-band voltages (V_{FB}) extracted in linear operation across (1) ambient, (2) $< 10^{-5}$ Torr vacuum, (3) 7 Torr water, and (4) 7 Torr pyridine saturated environments. (b) Corresponding $I_{D,\text{lin}}$ vs V_G traces at $V_D = 1 \text{ V}$ clearly show the large shifts between transitions, indicated by solid arrows. The constant slopes but changing intercept imply that only V_{FB} is affected by the medium. V_{FB} and $\mu_{\text{lin}}C_{\text{box}}$ were reproduced in vacuum after desorbing the molecules, confirming that the effects arise from physisorption and are reversible, as indicated by the dashed arrows.

in quite different values for V_{FB} [Fig. 2(a)] depending on the chemical state, as was the case in saturation. At $V_D = 1 \text{ V}$, the slope determination gives $\beta_{\text{lin}}^{(1)} = 11.00 \pm 0.03 \text{ } \mu\text{A/V}^2$, $\beta_{\text{lin}}^{(2)} = 10.40 \pm 0.02 \text{ } \mu\text{A/V}^2$, $\beta_{\text{lin}}^{(3)} = 10.60 \pm 0.02 \text{ } \mu\text{A/V}^2$, and $\beta_{\text{lin}}^{(4)} = 11.50 \pm 0.02 \text{ } \mu\text{A/V}^2$, corresponding to an average $\langle\beta_{\text{lin}}\rangle = 10.90 \pm 0.5 \text{ } \mu\text{A/V}^2$. This result is $\sim 17\%$ larger than the value for $\langle\beta_{\text{sat}}\rangle$ presented earlier, which can be understood by the lateral-field reduction of mobility μ_{sat} as compared to the low-field limit μ_{lin} .¹¹

Analogous to the similar gain factors obtained in saturation, the constant slopes in the triode regime show that the Ψ -MOSFET is primarily responding by changing V_{FB} instead of the field-effect mobility. After pyridine exposure and evacuation, the original characteristics were recovered in vacuum, indicating that the molecule does not induce irreversible changes to the H-terminated surface, namely, (2) \leftrightarrow (4) is a reversible process, as was similarly shown for water, (2) \leftrightarrow (3). The large -3.7 V shift in V_{FB} upon exposure to pyridine is similar to changes observed on silicon nanowire based FETs exposed to NH_3 vapor.²⁴

B. Estimating the adsorption induced surface charge

The change in V_{FB} induced by water and pyridine vapors is consistent with the adsorbates' inducing positive charge densities at the surface as observed previously.^{8,20} Downward band-bending induced by this positive charge draws electron density toward the surface, resulting in a shift of the threshold for accumulation (n -channel) to more negative values. These changes are further understood in terms of the field penetration depth in silicon. With $n_b \sim 10^{15} \text{ cm}^{-3}$, the

device layer thickness $d=150$ nm is on the order of the Debye length, $L_D=130$ nm, in the material. Therefore, adsorption-induced charges at the top film–vacuum interface produce fields capable of reaching the buried channel, modulating the conduction.

The absolute flat-band voltage is dependent on several parameters, including the work function difference between the substrate gate material and the Si film (φ_{MS}), the fixed/trapped and mobile charges in the buried oxide (Q_{box}) at the film–BOX interface, the capacitances of the film (C_{Si}) and buried oxide (C_{box}), the surface charge (Q_s), and the interface state density (D_{it2}) at the top film–vacuum interface,¹³ as expressed by Eq. (1):

$$V_{FB} = \varphi_{MS} - \frac{C_{Si}}{C_{box}(C_{Si} + qD_{it2})} Q_s - \frac{Q_{box}}{C_{box}}. \quad (1)$$

With respect to shifts in the flat-band voltage, most of these parameters are essentially unchanged during adsorption, except for the surface charge. Small variations, if any, in φ_{MS} , C_{Si} , C_{box} , and Q_{box} upon adsorption will contribute relatively less to V_{FB} as compared to changes in Q_s and D_{it2} . Moreover, we have already confirmed that the top interface state density D_{it2} of SOI-H is unchanged by the adsorption of water or pyridine, because the measurements are reversible after the gases are desorbed. Thus, if only Q_s changes and all other terms in the right-hand side of Eq. (1) are constant, then the shifts in the flat-band voltage (ΔV_{FB}) are proportional to the relative surface charge induced (ΔQ_s) by Eq. (2):

$$\Delta V_{FB} \approx -\alpha \cdot \Delta Q_s, \quad (2)$$

where $\alpha = C_{Si}/C_{box}(qD_{it2} + C_{Si})$. The device layer capacitance is $C_{Si} = \epsilon_0 \epsilon_{Si}/d$ with relative permittivity $\epsilon_{Si} = 11.9$. We have taken $D_{it2} = 1 \times 10^{10} \text{ eV}^{-1} \text{ cm}^{-2}$ for the H-terminated surface. Applying this approximation [Eq. (2)] to the data in Fig. 2 yields the following: $\Delta V_{2 \leftrightarrow 3} = |V_{FB,(3)} - V_{FB,(2)}| = 2.1$ V corresponds to $\Delta Q_{s,2 \leftrightarrow 3} = 1.2 \times 10^{11} \text{ cm}^{-2}$ between vacuum and water, and $\Delta V_{2 \leftrightarrow 4} = 3.7$ V corresponds to $\Delta Q_{s,2 \leftrightarrow 4} = 2.2 \times 10^{11} \text{ cm}^{-2}$ between vacuum and pyridine. These changes in surface charge density are comparable with those induced by pyridine and water adsorption derived from four-probe surface conductivity and Hall effect measurements.²⁰

C. Ambient oxidation changes V_{FB} irreversibly

In contrast to the reversible modulation demonstrated by water and pyridine adsorption, reactions on H-terminated Si can induce permanent surface states that cause the depletion of majority carriers and thereby irreversibly degrade the device performance. Hydrogen-terminated surfaces are known to oxidize slowly (over several days) in ambient atmosphere.^{25,26} Figure 3 illustrates the changes in V_{FB} of a SOI-H sample kept in ambient atmosphere as a function of time.

Drift is observable immediately after H-termination. Initially negative, V_{FB} is seen to change fairly rapidly, increasing by ~ 1 V in the first two hours. For longer exposures, the flat-band voltage continues to increase, crossing over from

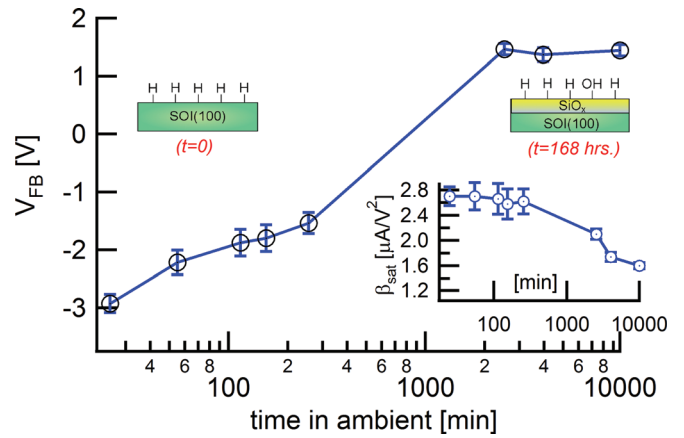


FIG. 3. (Color online) Evolution of V_{FB} for a Ψ -MOSFET on 200 nm SOI(100)-H (n -doped film/substrate) over seven days in ambient atmosphere. Corresponding changes in the gain factor β_{sat} are shown in the inset. As the surface incorporates oxygen, the creation of interface states significantly raises the flat-band voltage and decreases the effective electron mobility.

negative to positive values up to ~ 36 h, at which point it remains relatively constant. Quantitative interpretation of this shift is complicated because both the interface state density (due to oxidation) and the surface charge density (induced by water) change as the native oxide forms. Both processes affect the flat-band voltage and cannot be separated from each other in the present experiments.

Furthermore, the shapes of the $I_{D,sat}-V_G$ parabolas slowly change during this process, resulting in an overall reduction in β_{sat} by 40%, as shown in the inset of Fig. 3. The lowering of β_{sat} can be attributed to interface roughening as the surface incorporates oxygen with time, causing degradation of the effective mobility. The apparent mobility is initially found to be $390 \pm 25 \text{ cm}^2/\text{V} \cdot \text{s}$, assuming $f_g = 0.75$. Similar decreases in mobility associated with the surface roughness have been noted for methyl terminated SOI(111)- CH_3 surfaces.²⁷ Increasing contact resistance could additionally contribute to the observed mobility lowering. A useful feature of the Ψ -MOSFET configuration is the ability to monitor and separate changes in V_{FB} and β_{sat} at all times. Previously we combined sheet resistance and Hall effect measurements during the early stages of oxidation in order to separate the carrier density (decreasing with time) from the conductivity mobility (essentially constant) on SOI-H with a thickness of $1 \mu\text{m}$.⁸ However, at later stages of ambient oxidation the samples became increasingly resistive and did not produce good Hall effect measurements, whereas the pseudo-MOSFET could still be biased into accumulation suitably for parameter extraction. The present observations in Fig. 3 are in agreement with this previous work, confirming that degradation of the mobility is mostly observed at the later stages of oxidation (>8 h).

D. Gas phase alkylation of SOI(100)-H

In order to slow down the degradation of SOI-H caused by ambient oxidation that is demonstrated in the previous section, the surface can be passivated by molecular monolayers consisting of covalently attached alkyl chains. Most

commonly, solution-based methods involving the thermal or photochemical reaction of alkenes with H-terminated silicon are used to form these monolayers, rendering the surface more resistant to oxidation.^{28–30} In order to use the Ψ -MOS-FET technique to probe the changes induced by alkyl monolayer formation, we have chosen to employ a recently developed gas phase photochemical alkylation process.²¹ In this process, the absorption of 185 nm UV photons in the primary alkene $\text{CH}_3(\text{CH}_2)_k\text{CH}=\text{CH}_2(\text{g})$ induces photolysis, forming the reactive radical fragments needed to generate dangling bonds on the H-terminated surface (initiation). A radical chain reaction involving the direct reaction of the alkene itself with these dangling bonds can then propagate on the surface, forming the methyl terminated monolayer $\text{Si}-(\text{CH}_2)_{k+2}\text{CH}_3$. This approach is found to be ideally suited for forming monolayers on our SOI(100)-H pseudo-MOS-FETs. Particularly useful with respect to these measurements is that this process is compatible with prior EGaIn contact placement onto the freshly H-terminated SOI.

Because the previous report of alkyl monolayer formation using the gas phase photochemical route involved the use of atomically flat Si(111)-H substrates, it was necessary to fully characterize the monolayers formed on Si(100)-H surfaces using this process. Shown in Fig. 4 are the FTIR spectra of the freshly etched Si(100)-H surface before and after gas phase photochemical reaction with decene to form a Si-C10 surface.

The spectrum of the initial H-terminated surface is dominated by multiple silicon-hydrogen stretch modes. The integrated absorbance from 2070 to 2130 cm^{-1} is $\int A(\omega) - A_0(\omega) d\omega = 0.25 \text{ cm}^{-1} \pm 2\%$, an area routinely obtained after H-termination. An uncertainty level of 2% reflects the variability in area resulting from the inspection of several different baselines A_0 . There is a small degree of hydrocarbon contamination in the CH_x stretch region, 3000–2800 cm^{-1} , with an integrated absorbance area of $0.058 \text{ cm}^{-1} \pm 2\%$. Five distinct modes are visible at $\nu_{\text{as}}(\text{SiH}_3) = 2138 \text{ cm}^{-1}$, $\nu_{\text{as}}(\text{SiH}_2) = 2115 \text{ cm}^{-1}$, $\nu_{\text{s}}(\text{SiH}_2) = 2104 \text{ cm}^{-1}$, $\nu_{\text{as}}(\text{SiH}) = 2086 \text{ cm}^{-1}$, and $\nu_{\text{s}}(\text{SiH}) = 2073 \text{ cm}^{-1}$. The first in this series corresponds to the trihydride, the second and third to the asymmetric and sym-

metric dihydride, and the final two to the asymmetric and symmetric coupled monohydride stretch modes in rows.³¹

Upon reaction with 1-decene (top spectrum), these SiH_x modes appear as absorbance losses. This reflects the loss of hydrogen from the surface as a result of the reaction (because the H-terminated surface was used as the background). Quantitatively, this loss corresponds to an integrated absorbance of $-0.14 \text{ cm}^{-1} \pm 2\%$, or approximately half of the initial hydrogen signal. There is significant absorbance gain in the CH_x region, corresponding to an integrated area of $0.76 \text{ cm}^{-1} \pm 5\%$. The C10 monolayer exhibits four modes at $\nu_{\text{as}}(\text{CH}_3) = 2959 \text{ cm}^{-1}$, $\nu_{\text{as}}(\text{CH}_2) = 2922 \text{ cm}^{-1}$, $\nu_{\text{s}}(\text{CH}_3) = 2878 \text{ cm}^{-1}$, and $\nu_{\text{s}}(\text{CH}_2) = 2852 \text{ cm}^{-1}$, corresponding to methyl and methylene stretch vibrations of asymmetric and symmetric types.³² The position of the asymmetric methylene stretch at 2922 cm^{-1} indicates that the chains are reasonably well packed²⁸ and of a quality similar to that of monolayers formed using wet chemical methods with 1-decene on Si(111)-H.^{28,29} An absorbance maximum of 15.2 mAU (milliabsorbance units) is measured at this frequency. Correcting for the number of internal reflections (25) and the number of methylene units (9), this amounts to a contribution of 0.068 mAU/methylene, which is similar to values reported on Si(111)-H surfaces using solution phase methods.^{29,33}

Additional surface characterization of Si-C10 monolayers formed on moderately *n*-doped Si(100) wafer samples yielded ellipsometric thicknesses of $12 \pm 1 \text{ \AA}$ and static water contact angles of $100^\circ \pm 1^\circ$, similar to typical values reported for decyl monolayers on Si(100).³⁴ Most important, these monolayers were observed to have a small degree of band-bending into depletion, $50 \pm 15 \text{ mV}$, as measured by their surface photovoltage with an ambient Kelvin probe. For the carrier densities of the wafers used here ($n_b \sim 1 \times 10^{15} \text{ cm}^{-3}$), this corresponds to a net surface charge density of $Q_s = 2 \times 10^{10} \text{ cm}^{-2}$, demonstrating that the gas phase created monolayers produce electrically well-passivated interfaces.

The effects of forming a decyl monolayer on the SOI-H surface via the gas phase route have been studied using the pseudo-MOSFET as shown in Fig. 5. Good FET output characteristics are obtained for the C10 passivated surface, although the current at the same gate voltage is clearly reduced with respect to the SOI-H surface. From the parabolic fits in Fig. 5(b), the decyl termination is found to increase V_{FB} by $\sim 1.9 \text{ V}$ and decrease β_{sat} by 15%. The initial mobility on SOI-H was $\mu_{\text{sat}} = 1020 \pm 60 \text{ cm}^2/\text{V} \cdot \text{s}$.

Part of the observed shift in V_{FB} may be attributed to the creation of electrically active defect states associated with the reaction. The shift in V_{FB} and the small decrease in mobility are consistent with a slight degree of oxidation. However, the formation of the hydrophobic monolayer is also expected to reduce the coverage of adsorbed H_2O at the interface relative to SOI-H, which is shown in Sec. III A to have a non-negligible impact on the flat-band voltage determination. Therefore, some portion of the increase in V_{FB} is likely caused by (partial) displacement of water by the monolayer. The maximum contribution due to this displacement can be estimated by recalling from Figs. 1 and 2

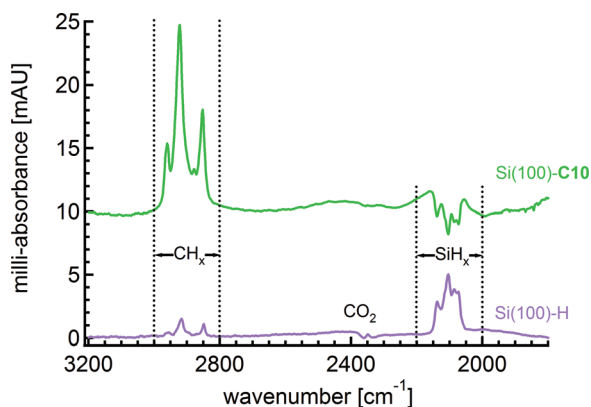


FIG. 4. (Color online) ATR-FTIR characterization of monolayer formation using the gas phase photochemical method of Eves *et al.* (Ref. 21). The spectra correspond to the initial HF-etched Si(100)-H surface (bottom) and the alkylated Si-C10 surface (top) formed by a radical chain reaction at 185 nm with 1-decene vapor.

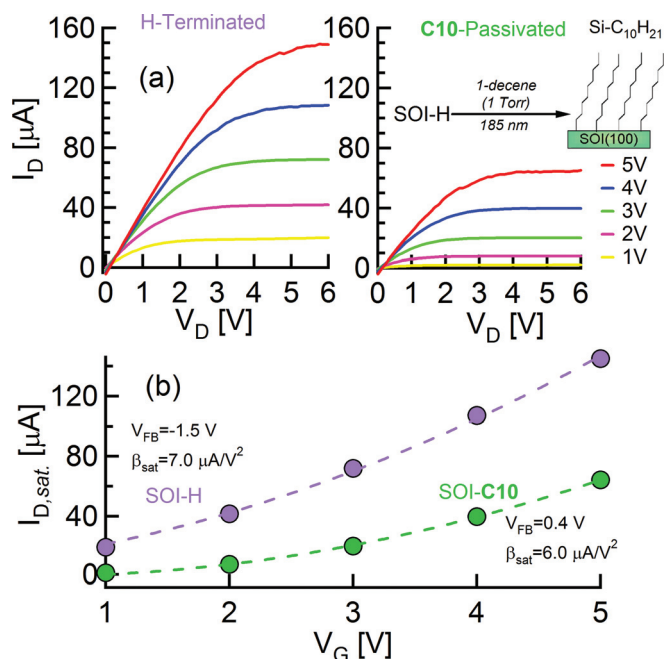


FIG. 5. (Color online) The effect of the covalent modification of 150 nm SOI(100)-H on the Ψ -MOSFET characteristics. (a) I_D - V_D characteristics measured in ambient atmosphere on the initial H-terminated surface and after the formation of a decyl monolayer SOI-C10 via a photochemical gas phase reaction. (b) Corresponding $I_{D,sat}$ - V_G curves, along with the parameters extracted from the parabolic fits, indicating changes in V_{FB} and β_{sat} .

that V_{FB} increases by ~ 0.5 V upon pumping SOI-H from ambient atmosphere to vacuum, corresponding to complete removal of surface bound H_2O . Consistency with Eq. (2) and the observed shifts in V_{FB} from -1.5 ± 0.1 V to 0.4 ± 0.1 V can be obtained by imposing reasonable estimates for D_{it2} (from $1.0 \times 10^{10} \text{ cm}^{-2} \text{ eV}^{-1}$ to $3.0 \times 10^{10} \text{ cm}^{-2} \text{ eV}^{-1}$) and Q_s (from $1.2 \times 10^{11} \text{ cm}^{-2}$ to $1.0 \times 10^{10} \text{ cm}^{-2}$). The cause and nature of interface state formation during this gas phase process have not been characterized.³⁵ A moderate shift in device characteristics associated with the modification reaction indicates that these monolayers largely preserve the low density of electrically active defects observed on the H-terminated surface, and suggests that they should form good passivating layers for molecular sensing applications.

Finally, we note that the gas phase photochemical process for alkyl monolayer formation used in the current work has a number of advantages as compared to traditional solution-based methods. These include shorter reaction times (minutes versus hours), more efficient use of the reagent, more systematic deoxygenating (freeze-pump-thawing versus rigorous bubbling in Ar), and no need for rinsing procedures that consume additional organic solvents. General drawbacks of this approach include its limited scope to alkenes with sufficiently high vapor pressure (Torr range), although this can be overcome by elevating the reaction temperature. Although the method works well for alkenes with an unreactive terminal group (such as the methyl-terminated layers studied here), the formation of functional monolayers with reactive groups suitable for subsequent attachment reactions remains a challenge.

IV. CONCLUSIONS AND PERSPECTIVES

In summary, the characteristics of the SOI-H Ψ -MOSFET have been shown to be highly sensitive to molecular adsorption and reaction events, and can be used to distinguish between reversible adsorption induced modulation as opposed to irreversible reaction induced changes. Appreciable top-gating action of the molecular adsorbates water and pyridine is shown to be highly reversible at room temperature and thus consistent with an adsorption induced charge transfer interaction. Such large shifts in the flat-band voltage caused by charge transfer from donor type molecules invites further experimental and theoretical investigations. Additionally, the influence of chemical modification can be probed systematically by use of a controlled gas phase alkylation process to form high quality ultrathin organic dielectrics on SOI-H. The passivation properties of these monolayers against oxidation and their response to the adsorption of molecular species are presently under investigation. These studies demonstrate the utility of the Ψ -MOSFET as a fast and simple approach for probing molecule-surface interactions on chemically modified silicon surfaces.

ACKNOWLEDGMENTS

G.P.L. and F.R. are grateful to NSERC (Discovery Grants) for partial funding of this work. F.R. acknowledges partial salary support from the Canada Research Chairs program. G.D. is grateful for the NRC GSSSP supplement.

- ¹R. Cohen, L. Kronik, A. Shanzer, D. Cahen, A. Liu, Y. Rosenwaks, J. K. Lorenz, and A. B. Ellis, *J. Am. Chem. Soc.* **121**, 10545 (1999).
- ²D. Cahen, R. Naaman, and Z. Vager, *Adv. Func. Mater.* **15**, 1571 (2005).
- ³G. P. Lopinski, B. J. Eves, O. Hul'ko, C. Mark, S. N. Patitsas, R. Boukherroub, and T. R. Ward, *Phys. Rev. B* **71**, 125308 (2005).
- ⁴O. Shaya, M. Shaked, A. Doron, A. Cohen, I. Levy, and Y. Rosenwaks, *Appl. Phys. Lett.* **93**, 043509 (2008).
- ⁵R. K. Hiremath, M. K. Rabinal, B. G. Mulimani, and I. M. Khazi, *Langmuir* **24**, 11300 (2008).
- ⁶G. Shalev, E. Halpern, A. Doron, A. Cohen, Y. Rosenwaks, and I. Levy, *J. Chem. Phys.* **131**, 024702 (2009).
- ⁷T. He, J. He, M. Lu, B. Chen, H. Pang, W. F. Reus, W. M. Nolte, D. P. Nackashi, P. D. Franzon, and J. M. Tour, *J. Am. Chem. Soc.* **128**, 14537 (2006).
- ⁸G. Dubey, G. P. Lopinski, and F. Rosei, *Appl. Phys. Lett.* **91**, 232111 (2007).
- ⁹S. A. Scott, W. Peng, A. M. Kiefer, H. Jiang, I. Knezevic, D. E. Savage, M. A. Eriksson, and M. G. Lagally, *ACS Nano* **3**, 1683 (2009).
- ¹⁰S. Cristoloveanu and S. Williams, *IEEE Electron. Device Lett.* **13**, 102 (1992).
- ¹¹S. Cristoloveanu, D. Munteanu, and M. S. T. Liu, *IEEE Trans. Electron. Devices* **47**, 1018 (2000).
- ¹²L. Hollt, M. Born, M. Schlosser, I. Eisele, J. Grabmeier, and A. Huber, *IEEE Trans. Electron. Devices* **54**, 2685 (2007).
- ¹³H. J. Hovel, *Solid-State Electron.* **47**, 1311 (2003).
- ¹⁴T. V. C. Rao, J. Antoszewski, L. Faraone, S. Cristoloveanu, T. Nguyen, P. Gentil, N. Bresson, and F. Allibert, *J. Appl. Phys.* **103**, 034503 (2008).
- ¹⁵G. M. Laws, T. J. Thornton, J. Yang, L. De la Garza, M. Kozicki, and D. Gust, *Phys. Status Solidi B* **233**, 83 (2002).
- ¹⁶T. He, A. Corley, M. Lu, N. H. Di Spigna, J. He, D. P. Nackashi, P. D. Franzon, and J. M. Tour, *J. Am. Chem. Soc.* **131**, 10023 (2009).
- ¹⁷T. He, M. Lu, J. Yao, J. He, B. Chen, N. H. Di Spigna, D. P. Nackashi, P. D. Franzon, and J. M. Tour, *Adv. Mater.* **20**, 4541 (2008).
- ¹⁸On the 150 nm nominally *p*-doped SOI substrates, Hall effect measurements indicated *n*-type conduction in the top silicon layer, a common occurrence for *p*-type SIMOX wafers that is known to arise from the formation of oxygen related donors at the BOX interface.

- ¹⁹When large gate leakage currents were encountered, the samples were discarded. Sidewall leakage from the Si film edge to the substrate was suspected.
- ²⁰G. Dubey, F. Rosei, and G. P. Lopinski, *Small* **6**, 2892 (2010).
- ²¹B. J. Eves and G. P. Lopinski, *Langmuir* **22**, 3180 (2006).
- ²²M. Morita, T. Ohmi, E. Hasegawa, M. Kawakami, and M. Ohwada, *J. Appl. Phys.* **68**, 1272 (1990).
- ²³High resolution energy loss spectroscopy spectra of H-terminated samples obtained in the course of this study show no evidence of oxidation after 7 h of exposure to H₂O under conditions similar to those for the electrical measurements.
- ²⁴A. A. Talin, L. L. Hunter, F. Leonard, and B. Rokad, *Appl. Phys. Lett.* **89**, 153102 (2006).
- ²⁵D. Graf, M. Grudner, and R. Schulz, *J. Appl. Phys.* **68**, 5155 (1990).
- ²⁶M. R. Houston and R. Maboudian, *J. Appl. Phys.* **78**, 3801 (1995).
- ²⁷J. E. Green, S. J. Wong, and J. R. Heath, *J. Phys. Chem. C* **112**, 5185 (2008).
- ²⁸M. R. Linford, P. Fenter, P. M. Eisenberger, and C. E. D. Chidsey, *J. Am. Chem. Soc.* **117**, 3145 (1995).
- ²⁹R. Boukherroub, S. Morin, F. Bensebaa, and D. D. M. Wayner, *Langmuir* **15**, 3831 (1999).
- ³⁰R. T. W. Popoff, H. Asanuma, and H.-Z. Yu, *J. Phys. Chem. C* **114**, 10866 (2010).
- ³¹P. Dumas, Y. J. Chabal, and P. Jakob, *Surf. Sci.* **269**, 867 (1992).
- ³²M. D. Porter, T. B. Bright, D. L. Allara, and C. E. D. Chidsey, *J. Am. Chem. Soc.* **109**, 3559 (1987).
- ³³T. K. Mischki, G. P. Lopinski, and D. D. M. Wayner, *Langmuir* **25**, 5626 (2009).
- ³⁴E. J. Faber, L. C. P. M. de Smet, W. Olthuis, H. Zuilhof, E. J. R. Sudhölter, P. Bergveld, and A. van den Berg, *ChemPhysChem* **6**, 2153 (2005).
- ³⁵These might be related to impurities in the decene solution or oxygen present in the background pressure of the chamber, in which case the process could be optimized. They might also originate from the generation of a small density of uncapped dangling bonds (mid-gap states) during the chain reaction.